

Sparse Bayesian Learning Based DOA Estimation and Array Gain-Phase Error Self-Calibration

Zili Li and Zhao Huang*

Abstract—This paper proposes a joint estimation algorithm based on sparse-Bayesian learning (SBL) for the gain-phase problem between array antenna channels. The algorithm uses the idea of the iterative method to jointly estimate the direction-of-arrival (DOA) and gain-phase error calibration coefficients in the iterative process, combining self-calibration and calibration with a calibration source. At each iteration, the rough value of DOA is first estimated using SBL, and then the DOA estimate is used to calculate the gain-phase error calibration coefficient. The value obtained in each iteration is brought into the error cost function, which is constructed based on the principle of signal and noise subspace orthogonality. Iterations are continued until convergence to find the minimum value of the cost function. The algorithm does not require a priori knowledge of array perturbations and has good performance in DOA and array gain and phase error estimation. Simulations and experimental measurements show that the method has better calibration performance than other methods based on optimization algorithms, and the algorithm effectively improves the antenna gain.

1. INTRODUCTION

In recent years, most scholars have devoted themselves to estimating far-field signal direction using array signal processing techniques [1–3]. In practical engineering applications, when array radar is used to calculate the DOA, deviations between antenna units inevitably lead to inaccurate radar detection targets in complex backgrounds [4]. Therefore, the error correction of an array antenna is an essential part of radar array signal processing.

Array error correction can be usually divided into array element mutual coupling effect correction [5], array gain and phase error correction [6, 7], array element position correction, and array directional map correction. The commonly used error correction methods are divided into two main categories based on the presence or absence of a calibration source. Calibration with a calibration source is done by setting up a spatially accurate known additional source for the offline estimation of the error parameters. This type of method requires a particular auxiliary source, and setting up another source also increases the cost of the measurement system. The self-calibration does not require an additional calibration source but mainly uses a specific optimization function to jointly estimate the error parameters of the spatial source orientation and the array. The algorithm in [8, 9] uses a sensor feature structure-based orientation method and an error calibration algorithm. The algorithm in [10] uses genetic algorithm (GA) calibration of array deviation and orientation measurement. The algorithm in [11] uses a particle swarm optimization (PSO) algorithm to calibrate some arrays' gain and phase errors. Calibration source correction methods have the advantages of low cost and simple operation compared to self-calibration techniques. Still, they are not easy to obtain the optimal solution when solving error parameters iteratively. They are prone to fall into local optimality and have high request initial values for the iterations. To address the above limitations in calibration without calibration

Received 30 December 2021, Accepted 7 February 2022, Scheduled 15 February 2022

* Corresponding author: Zhao Huang (zhaoh_cs@sina.com).

The authors are with the School of Electronic Engineering, Guangxi Normal University, Guilin 541004, China.

sources, SBL algorithms, initially proposed in compressive sensing theory [12,13], are subsequently introduced into the field of array signal processing and used to solve DOA estimation and errors correction in array signal processing [14–16]. The sparse reconstruction algorithm is used to recover the signal to reduce the number of samples, data transmission, storage, and processing cost of the signal and improve the parameter estimability. While using the SBL algorithm for DOA estimation overcomes the shortcomings of traditional DOA estimation algorithm, because SBL algorithm utilizes statistical optimization, it makes the algorithm fast in computation, robust and accurate in estimation.

While using the SBL algorithm for DOA estimation overcomes the shortcomings of traditional DOA estimation algorithm, because SBL algorithm utilizes statistical optimization, it makes the algorithm fast in computation, robust and accurate in estimation

In this paper, an SBL algorithm-based self-calibration algorithm for array gain-phase error is proposed for the problem of inconsistent gain-phase response among array elements. Based on the principle of signal and noise subspace orthogonality, it constructs the error cost function and iteratively solves for the function's extreme value. Use the sparsity of DOA in the null domain and the SBL method to estimate the DOA in each iteration. Then the DOA estimation results are used to solve for the deviation parameters. The experimental results show that the proposed algorithm effectively improves the efficiency and accuracy of passive calibration compared with other classical array error calibration algorithms.

2. SIGNAL MODEL

2.1. Array Error Model

Assume that there are K far-field uncorrelated narrowband signals incident to an L -element uniform linear array (ULA) with an array spacing of half wavelength, i.e., $d = \lambda/2$, where λ denotes the wavelength of the received signal, and the directions of arrival of the signals are $\theta = [\theta_1, \dots, \theta_K]$, where $\theta_k \in [-\pi/2, \pi/2]$. When the gain-phase errors exist, the complex-valued baseband signal received by the ULA at a time t can be expressed as

$$\mathbf{x}(t) = \mathbf{\Gamma} \mathbf{A}(\theta) \mathbf{s}(t) + \mathbf{E}(t) \quad (1)$$

where the matrix is an array manifold matrix; $\mathbf{a}(\theta_k) = [1, e^{-j\pi \sin \theta_k}, \dots, e^{-j\pi(L-1) \sin \theta_k}]^T \in \mathbb{C}^{L \times 1}$ is the steering vector of the k th source; $\mathbf{s}(t) = [s_1(t), \dots, s_K(t)]^T \in \mathbb{C}^{K \times 1}$ is the source signal complex envelope; $\mathbf{E}(t)$ is the $L \times 1$ dimensional Gaussian white noise; $\mathbf{\Gamma} = \text{diag}(\alpha_1 e^{-j\phi_1}, \dots, \alpha_L e^{-j\phi_L}) \in \mathbb{C}^{L \times L}$ is the array gain-phase error vector. α_l and ϕ_l denote the gain and phase error of the l th sensor, respectively, where $\alpha_1 = 1, \phi_1 = 0$. Express Equation (1) in matrix form as

$$\mathbf{X} = \mathbf{\Gamma} \mathbf{A}(\theta) \mathbf{S} + \mathbf{E} \quad (2)$$

where $\mathbf{X} \in \mathbb{C}^{L \times N}$ denotes the array receive matrix at N snapshot moments; $\mathbf{S} \in \mathbb{C}^{K \times N}$ denotes the source signal complex envelope; $\mathbf{E} \in \mathbb{C}^{L \times N}$ denotes the observation noise matrix.

2.2. Array Error Sparse Signal Model

Consider the range of possible incoming directions of the signal in space $[-90^\circ, 90^\circ]$ divided into M grids at equal intervals, with each grid point representing a possible direction of incidence, then the super-complete set of signal incidence angles is obtained, i.e., $\tilde{\theta} = [\tilde{\theta}_1, \dots, \tilde{\theta}_M]$. Therefore, Equation (1) can be written in a sparse representation as

$$\mathbf{x}(t) = \mathbf{\Gamma} \mathbf{A}(\tilde{\theta}) \tilde{\mathbf{s}}(t) + \mathbf{E}(t) \quad (3)$$

where $\mathbf{A}(\tilde{\theta}) = [\mathbf{a}(\tilde{\theta}_1), \dots, \mathbf{a}(\tilde{\theta}_M)] \in \mathbb{C}^{L \times M}$ is the over-complete array manifold matrix; $\tilde{\mathbf{s}}(t) = [\tilde{s}_1, \dots, \tilde{s}_M] \in \mathbb{C}^{M \times 1}$ is the source signal complex envelope. The number of sources K generally incident to the sensor array is much smaller than the set of possible incident azimuths M . Assuming a fixed angle of incidence of the signal, then only when $\theta_k = \tilde{\theta}_m$, the elements of the m th row of $\tilde{\mathbf{s}}(t)$ are non-zero. From $K \ll M$, we know that $\tilde{\mathbf{s}}(t)$ has row sparsity. By abbreviating $\mathbf{\Gamma} \mathbf{A}(\tilde{\theta})$ to $\tilde{\mathbf{A}}$, and Equation (3) can be written in matrix form as

$$\mathbf{X} = \tilde{\mathbf{A}} \tilde{\mathbf{S}} + \mathbf{E} \quad (4)$$

where $\tilde{\mathbf{S}} \in \mathbb{C}^{M \times N}$ denotes the source signal complex envelope and with row sparsity.

2.3. Reduced-dimensional Signal Model

In order to reduce the data scale and computation, the singular-value-decomposition (SVD) [17] is used to reduce the dimensionality of the array reception matrix \mathbf{X} . In addition to reducing the data scale, SVD also accumulates the signal energy and separates the noise, thus improving the algorithm's robustness under low signal-to-noise ratio (SNR) conditions. Assuming that $\mathbf{X} = \mathbf{U}\mathbf{\Sigma}\mathbf{V}^T/\sqrt{N}$, then the sparse representation problem of Equation (4) can be simplified as

$$\mathbf{X}_{SV} = \tilde{\mathbf{A}}\tilde{\mathbf{S}}_{SV} + \mathbf{E}_{SV} \quad (5)$$

where $\mathbf{X}_{SV} = \mathbf{X}\mathbf{V}\mathbf{D}$, $\tilde{\mathbf{S}}_{SV} = \tilde{\mathbf{S}}\mathbf{V}\mathbf{D}$, $\mathbf{E}_{SV} = \mathbf{E}\mathbf{V}\mathbf{D}$, and $\mathbf{D} = [\mathbf{I}_K, \mathbf{0}]^T$, \mathbf{I}_K denotes the K-dimensional unit matrix.

3. DOA ESTIMATION PRINCIPLE USING SBL

From the above analysis, we know that $\tilde{\mathbf{S}}_{SV}$ has row sparsity, so the DOA can be estimated by calculating the position of the non-zero row in $\tilde{\mathbf{S}}_{SV}$. Assume that each column of the array observation noise matrix \mathbf{N}_{SV} obeys a Gaussian distribution with mean zero and variance equal to σ_n^2 . The columns are uncorrelated with each other. Then the array received signal \mathbf{X}_{SV} obeys a posteriori Gaussian distribution with mean equal to $\tilde{\mathbf{A}}\tilde{\mathbf{S}}_{SV}$ and variance equal to $\sigma_e^2 = \sigma_n^2/N$, i.e.,

$$p(\mathbf{X}_{SV} | \tilde{\mathbf{S}}_{SV}; \sigma_e^2) = (2\pi\sigma_e^2)^{-\frac{LK}{2}} \exp\left(-\frac{1}{2\sigma_e^2} \|\mathbf{X}_{SV} - \tilde{\mathbf{A}}\tilde{\mathbf{S}}_{SV}\|_F^2\right) \quad (6)$$

According to the automatic relevance determination (ARD) principle [18], set a prior distribution modulated by a hyperparameter vector $\tau = [\tau_1, \dots, \tau_M]^T$, which controls the previous variance of each row of $\tilde{\mathbf{S}}_{SV}$. Then each row of $\tilde{\mathbf{S}}_{SV}$ follows a Gaussian prior distribution:

$$p(\tilde{\mathbf{S}}_{SV}(m, :); \tau) = (2\pi\tau_m)^{-\frac{K}{2}} \exp\left(-\frac{\|\tilde{\mathbf{S}}_{SV}(m, :)\|_2^2}{2\tau_m}\right) \quad (7)$$

where $\tilde{\mathbf{S}}_{SV}(m, :)$ denotes the element of the m th row of $\tilde{\mathbf{S}}_{SV}$. When all the elements of that row are zero, the τ_m value is zero, and when the elements of the row are not all zero, the τ_m value is not zero, which shows that τ has sparsity. According to the fact that the rows of $\tilde{\mathbf{S}}_{SV}$ are not correlated with each other, we can get

$$\begin{aligned} p(\tilde{\mathbf{S}}_{SV}; \tau) &= \prod_{m=1}^M p(\tilde{\mathbf{S}}_{SV}(m, :); \tau_m) \\ &= [(2\pi)^M |\mathbf{\Lambda}|]^{-\frac{K}{2}} \exp\left(-\frac{1}{2} \tilde{\mathbf{S}}_{SV}^H \mathbf{\Lambda}^{-1} \tilde{\mathbf{S}}_{SV}\right) \end{aligned} \quad (8)$$

where $(\cdot)^H$ denote the Hermitian operations of a matrix or a vector, $\mathbf{\Lambda} = \text{diag}(\tau)$.

According to the full probability formula, the probability density function of the received signal of the array is

$$\begin{aligned} p(\mathbf{X}_{SV}; \tau, \sigma_e^2) &= \int p(\mathbf{X}_{SV} | \tilde{\mathbf{S}}_{SV}; \sigma_e^2) p(\tilde{\mathbf{S}}_{SV}; \tau) d\tilde{\mathbf{S}}_{SV} \\ &= C * \exp\left\{-\frac{1}{2\sigma_e^2} \mathbf{X}_{SV}^H \left[\mathbf{I}_L - \tilde{\mathbf{A}} \left(\tilde{\mathbf{A}}^H \tilde{\mathbf{A}} + \sigma_e^2 \mathbf{\Lambda}^{-1}\right)^{-1} \tilde{\mathbf{A}}^H\right] \mathbf{X}_{SV}\right\} \end{aligned} \quad (9)$$

where C denotes the constant, and \mathbf{I}_L denotes the L-dimensional unit matrix. It can be seen that the received signal \mathbf{X}_{SV} obeys a Gaussian distribution with mean equal to zero, and the covariance matrix $\mathbf{\Sigma}_{\mathbf{X}_{SV}}$ satisfies

$$\mathbf{\Sigma}_{\mathbf{X}_{SV}}^{-1} = \frac{1}{\sigma_e^2} \left[\mathbf{I}_L - \tilde{\mathbf{A}} \left(\tilde{\mathbf{A}}^H \tilde{\mathbf{A}} + \sigma_e^2 \mathbf{\Lambda}^{-1}\right)^{-1} \tilde{\mathbf{A}}^H\right] \quad (10)$$

According to the matrix inverse formula $(A + BCD)^{-1} = A^{-1} - A^{-1}BC(I + DA^{-1}BC)^{-1}DA^{-1}$, we can get

$$\Sigma_{\mathbf{X}_{SV}} = \sigma_e^2 \mathbf{I} + \tilde{\mathbf{A}} \Lambda \tilde{\mathbf{A}}^H \quad (11)$$

The posterior probability of the source signal $\tilde{\mathbf{S}}_{SV}$ about the received signal of the array can be expressed according to the Bayesian formula as

$$\begin{aligned} p(\tilde{\mathbf{S}}_{SV} | \mathbf{X}_{SV}; \tau) &= \frac{p(\mathbf{X}_{SV} | \tilde{\mathbf{S}}_{SV}; \sigma_e^2) p(\tilde{\mathbf{S}}_{SV}; \tau)}{p(\mathbf{X}_{SV}; \tau, \sigma_e^2)} \\ &= C * \exp\left(-\frac{1}{2\sigma_e^2} \left\| \mathbf{X}_{SV} - \tilde{\mathbf{A}} \tilde{\mathbf{S}}_{SV} \right\|_F^2 - \frac{1}{2} \tilde{\mathbf{S}}_{SV}^H \Lambda^{-1} \tilde{\mathbf{S}}_{SV} + \frac{1}{2} \mathbf{X}_{SV}^H \Sigma_{\mathbf{X}_{SV}}^{-1} \mathbf{X}_{SV}\right) \end{aligned} \quad (12)$$

According to Equation (12), the mean of the source signal $\tilde{\mathbf{S}}_{SV}$ is the zero of the first-order derivative of the exponential part of Equation concerning $\tilde{\mathbf{S}}_{SV}$. The inverse of the covariance matrix is the second-order derivative of the exponential function concerning $\tilde{\mathbf{S}}_{SV}$ [19]. Denoting the exponential part of Equation (12) as F , it can be made that

$$\begin{aligned} F &= \frac{1}{2\sigma_e^2} \left\| \mathbf{X}_{SV} - \tilde{\mathbf{A}} \tilde{\mathbf{S}}_{SV} \right\|_F^2 - \frac{1}{2} \tilde{\mathbf{S}}_{SV}^H \Lambda^{-1} \tilde{\mathbf{S}}_{SV} + \frac{1}{2} \mathbf{X}_{SV}^H \Sigma_{\mathbf{X}_{SV}}^{-1} \mathbf{X}_{SV} \\ &= \frac{1}{2\sigma_e^2} \left[\tilde{\mathbf{S}}_{SV}^H \left(\tilde{\mathbf{A}}^H \tilde{\mathbf{A}} + \sigma_e^2 \Lambda^{-1} \right) \tilde{\mathbf{S}}_{SV} - \mathbf{X}_{SV}^H \tilde{\mathbf{A}} \tilde{\mathbf{S}}_{SV} - \tilde{\mathbf{S}}_{SV}^H \tilde{\mathbf{A}}^H \mathbf{X}_{SV} + \mathbf{X}_{SV}^H \mathbf{X}_{SV} \right] + \frac{1}{2} \mathbf{X}_{SV}^H \Sigma_{\mathbf{X}_{SV}}^{-1} \mathbf{X}_{SV} \end{aligned} \quad (13)$$

Finding the first-order derivative of $\tilde{\mathbf{S}}_{SV}$ with respect to F yields

$$\frac{dF}{d\tilde{\mathbf{S}}_{SV}} = \frac{1}{2\sigma_e^2} \left[2 \left(\tilde{\mathbf{A}}^H \tilde{\mathbf{A}} + \sigma_e^2 \Lambda^{-1} \right) \tilde{\mathbf{S}}_{SV} - 2 \tilde{\mathbf{A}}^H \mathbf{X}_{SV} \right] \quad (14)$$

Finding the second order derivative of $\tilde{\mathbf{S}}_{SV}$ with respect to F , we get

$$\frac{d^2 F}{d\tilde{\mathbf{S}}_{SV}^2} = \frac{1}{\sigma_e^2} \left(\tilde{\mathbf{A}}^H \tilde{\mathbf{A}} + \sigma_e^2 \Lambda^{-1} \right) \quad (15)$$

Let $dF/d\tilde{\mathbf{S}}_{SV} = 0$ to obtain

$$\begin{aligned} \mu_{\tilde{\mathbf{S}}_{SV}} &= \left(\tilde{\mathbf{A}}^H \tilde{\mathbf{A}} + \sigma_e^2 \Lambda^{-1} \right)^{-1} \tilde{\mathbf{A}}^H \mathbf{X}_{SV} \\ &= \Lambda \tilde{\mathbf{A}}^H \Sigma_{\mathbf{X}_{SV}}^{-1} \mathbf{X}_{SV} \end{aligned} \quad (16)$$

From the above analysis, we can obtain

$$\Sigma_{\tilde{\mathbf{S}}_{SV}}^{-1} = \frac{1}{\sigma_e^2} \tilde{\mathbf{A}}^H \tilde{\mathbf{A}} + \Lambda^{-1} \quad (17)$$

where $\mu_{\tilde{\mathbf{S}}_{SV}}$ denotes the mean of the posterior Gaussian distribution obeyed by $\tilde{\mathbf{S}}_{SV}$. $\Sigma_{\tilde{\mathbf{S}}_{SV}}^{-1}$ denotes the inverse of the covariance matrix, and applying the matrix inverse formula can transform Equation (17) into

$$\Sigma_{\tilde{\mathbf{S}}_{SV}} = \Lambda - \Lambda \tilde{\mathbf{A}}^H \Sigma_{\mathbf{X}_{SV}}^{-1} \tilde{\mathbf{A}} \Lambda \quad (18)$$

From the above analysis, it can be seen that $\tilde{\mathbf{S}}_{SV}$ can be regarded as a redundant parameter, and it is only necessary to determine the position of the non-zero element in τ to determine the azimuth angle of the incident signal. Based on the ARD principle to construct the cost function L

$$L(\tau, \sigma_e^2) \triangleq K \log |\Sigma_{\mathbf{X}_{SV}}| + \sum_{k=1}^K \mathbf{X}_{SV}^T(:, k) \Sigma_{\mathbf{X}_{SV}}^{-1} \mathbf{X}_{SV}(:, k) \quad (19)$$

Therefore, by minimizing the cost function equation, the sparse vector τ and noise variance σ_e^2 can be obtained. The minimum value of the cost function is solved iteratively using the expectation-maximization (EM) algorithm [20], whose iteration formula for step i is

$$\begin{aligned} \tau_m^{i+1} &= \frac{(1/K) \left\| \mu_{\tilde{\mathbf{s}}_{SV}}(m, :) \right\|_2^2}{1 - (\tau_m^{(i)})^{-1} \left(\boldsymbol{\Sigma}_{\tilde{\mathbf{s}}_{SV}} \right)_{mm}^{(i)}}, \quad \forall m = 1, \dots, M \\ (\sigma_e^2)^{(i+1)} &= \frac{(1/K) \left\| \mathbf{X}_{SV} - \tilde{\mathbf{A}} \tilde{\mathbf{S}}_{SV} \right\|_F^2}{L - M + \sum_{m=1}^M (\tau_m^{(i)})^{-1} \left(\boldsymbol{\Sigma}_{\tilde{\mathbf{s}}_{SV}} \right)_{mm}^{(i)}} \end{aligned}$$

where $\mu_{\tilde{\mathbf{s}}_{SV}}(m, :)$ denotes the element in the m th row of $\mu_{\tilde{\mathbf{s}}_{SV}}$, and $(\boldsymbol{\Sigma}_{\tilde{\mathbf{s}}_{SV}})_{mm}$ denotes the element on the diagonal of the m th row of $\boldsymbol{\Sigma}_{\tilde{\mathbf{s}}_{SV}}$. The initial value of σ_e^2 can be obtained by averaging the smaller singular values of \mathbf{X} .

4. DAIN-PHASE ERROR CORRECTION PARAMETER ESTIMATION ALGORITHM

After the rough estimation of DOA is obtained by the above SBL algorithm, the results of the angle estimation are used to calibrate the array gain-phase deviation. Assume that the DOA estimation results are $\hat{\theta} = [\hat{\theta}_1, \dots, \hat{\theta}_K]$. The covariance matrix of the array signal is found on the basis of Equation (2) as

$$\mathbf{R}_X = E [\mathbf{X}\mathbf{X}^H] \tag{20}$$

The feature decomposition is performed on \mathbf{R}_X ; the feature values are arranged in descending order; the space tended by the smaller $L - K$ feature values corresponding to the feature vectors constitutes the noise subspace, denoted as $\mathbf{U}_N = [\mathbf{u}_{k+1}, \mathbf{u}_{k+2}, \dots, \mathbf{u}_L]$, using the principle that the signal subspace and noise subspace are orthogonal to each other, constructing the cost function \tilde{J}

$$\begin{aligned} \tilde{J} &= \sum_{k=1}^K \left\| \mathbf{U}_N^H \boldsymbol{\Gamma} \mathbf{a}(\hat{\theta}_k) \right\|^2 \\ &= \sum_{k=1}^K \mathbf{a}(\hat{\theta}_k)^H \boldsymbol{\Gamma}^H \mathbf{U}_N \mathbf{U}_N^H \boldsymbol{\Gamma} \mathbf{a}(\hat{\theta}_k) \end{aligned} \tag{21}$$

then the value of $\boldsymbol{\Gamma}$ can be obtained by minimizing \tilde{J} .

According to the Lemma in the literature [9], for any $L * 1$ complex vector $\mathbf{a}(\hat{\theta}_k)$ and any $L * L$ complex diagonal matrix $\boldsymbol{\Gamma}$, we can obtain

$$\boldsymbol{\Gamma} \mathbf{a}(\hat{\theta}_k) = \tilde{\mathbf{a}}(\hat{\theta}_k) \boldsymbol{\gamma} \tag{22}$$

where $\tilde{\mathbf{a}}(\hat{\theta}_k) = \text{diag}(\mathbf{a}(\hat{\theta}_k))$ and $\boldsymbol{\gamma}$ is a vector consisting of the elements on the main diagonal of the complex diagonal matrix $\boldsymbol{\Gamma}$, i.e., $\gamma_i = \boldsymbol{\Gamma}_{ii}$. Thus, by the Lemma, Equation (21) can be rewritten as

$$\tilde{J} = \boldsymbol{\gamma}^H \left\{ \sum_{k=1}^K \tilde{\mathbf{a}}(\hat{\theta}_k^{(i)})^H \mathbf{U}_N \mathbf{U}_N^H \tilde{\mathbf{a}}(\hat{\theta}_k^{(i)}) \right\} \boldsymbol{\gamma} \tag{23}$$

Since the first array element is used as a reference, Equation (23) is minimized under the constraint, $\boldsymbol{\gamma}^H \mathbf{w} = 1$, $\mathbf{w} = [1, 0, 0, \dots, 0]^T$. Its iterative formula is

$$\boldsymbol{\gamma}^{(i+1)} = \frac{(\mathbf{D}^{(i)})^{-1} \mathbf{w}}{\mathbf{w}^T (\mathbf{D}^{(i)})^{-1} \mathbf{w}} \tag{24}$$

where $\mathbf{D}^{(i)} = \sum_{k=1}^K \tilde{\mathbf{a}}(\hat{\theta}_k^{(i)})^H \mathbf{U}_N \mathbf{U}_N^H \tilde{\mathbf{a}}(\hat{\theta}_k^{(i)})$

The main steps of the proposed algorithm are summarized in Algorithm 1.

Algorithm 1. proposed algorithm flow

Pre-processing Sparse representation of the received signal X of the array;

Initialization $i=0$, $\mathbf{\Gamma}^{(i)} = \mathbf{\Gamma}_0 \mathbf{\Gamma}_0$ can be based on regular gain and phase values or arbitrary random complex numbers;

Step 1 The dimensionality reduction of X , denoted as X_{SV} . Estimate the DOA using SBL algorithm to obtain the guidance vector of the array manifold matrix $\mathbf{A}(\hat{\theta}^{(i)}) = [\mathbf{a}(\hat{\theta}_1^{(i)}), \dots, \mathbf{a}(\hat{\theta}_K^{(i)})]$;

Step 2 Update the value of the error parameter $\gamma^{(i+1)}$ according to Equation (24);

Step 3 Calculate the value of the cost function $\tilde{J}^{(i)}$ according to Equation (23);

Step 4 If $\tilde{J}^{(i-1)} - \tilde{J}^{(i)} > \varepsilon$ (a preset threshold) then $X = X * \mathbf{\Gamma}$, $i = i + 1$, go to step 1. If $\tilde{J}^{(i-1)} - \tilde{J}^{(i)} \leq \varepsilon$, done.

5. EXPERIMENTS AND ANALYSIS

Based on the algorithm proposed in this paper, simulation experiments were conducted on the computer. In each simulation experiment, the array is assumed to be a ULA with elements L and the element spacing half a wavelength. The estimated signal source is a far-field narrowband signal; the noise is additive Gaussian white noise; and the number of snapshots is N . The gain-phase deviation coefficients $\mathbf{\Gamma}$ of the array in each simulation are randomly generated by $\alpha_i \in (0.5, 1.5)$ and $\phi_i \in (-\pi/6, \pi/6)$, respectively. The SNR is defined as $10 \lg(\sigma_s^2/\sigma_n^2)$, where σ_s^2 and σ_n^2 indicate the signal power and noise power, respectively. In the experiments, the grid interval of the airspace division for DOA estimation using SBL is 2° in all cases.

5.1. Effectiveness of the Proposed Algorithm

A ULA with half-wavelength array spacing is considered, which is composed of 16 sensors, and the three incoherent sources with unknown incident direction are 1° , 7° and 22° , respectively. The SNR is 5 dB, and the number of snapshots is 512. The MUSIC power spectra of the signal before and after correction are shown in Figure 1.

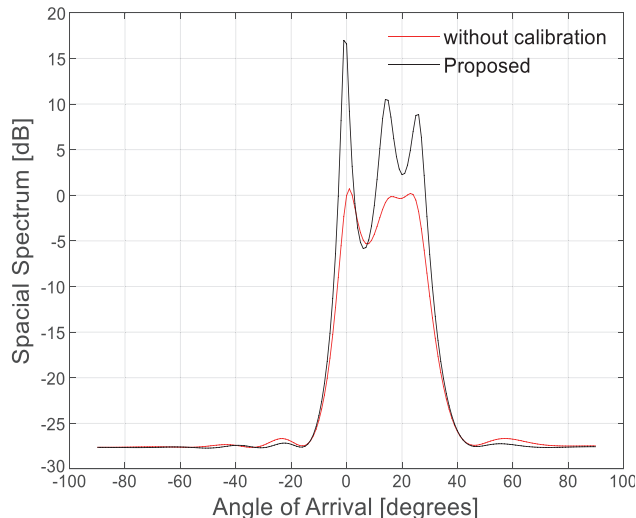


Figure 1. The comparison between before calibration and after calibration.

From Figure 1, we can see that the MUSIC spatial spectrum is relatively flat, and the information of the spectral peaks is weak due to the gain-phase errors before correction. After correction, the spectral peaks rise significantly. All DOAs can be obtained accurately, indicating that the channel correction effectively improves the SNR, and the performance of DOA estimation is improved dramatically.

5.2. Performance Comparison

A ULA with 16 sensors is considered, and the spacing of array elements is half wavelength, and the number of snapshots is 512. Any three equal-power uncorrelated narrowband signals in space are incident on the planar array during each experiment. The root mean square error (RMSE) is defined as

$$RMSE = \frac{1}{K} \sum_{k=1}^K \sqrt{\frac{1}{T} \sum_{t=1}^T (\hat{\theta}_{kt} - \theta_k)^2} \tag{25}$$

where T is the number of independent Monte Carlo experiments; K is the number of sources; θ_k is the actual value of DOA of the k th source, and $\hat{\theta}_{kt}$ is the estimated value of the pair obtained from the t th Monte Carlo experiment.

Based on 100 Monte Carlo experiments, the proposed method is compared with gain-phase error calibration based on, GA [10], PSO [11], respectively, and traditional feature structure-based orientation correction method [9]. The results of DOA estimation with different SNRs are shown in Figure 2. The average operation time of the algorithm is shown in Figure 3.

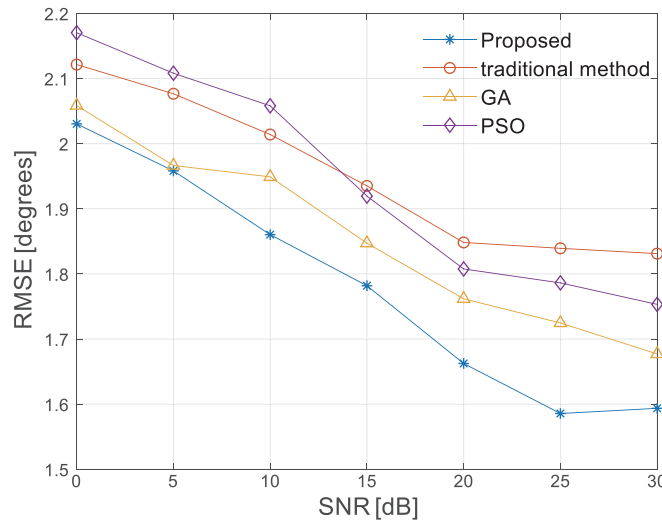


Figure 2. Estimated RMSE of DOA with different SNRs.

From Figure 2, it can be seen that the DOA estimation errors after calibration of the four methods at different SNRs do not exceed 2.2°, among which the algorithm of this paper has the most superior performance, indicating that the algorithm can effectively suppress the influence of noise in the array. The DOA can be accurately obtained from the corrected data when the gain-phase deviation exists in the array. From Figure 3, we can see that the algorithm of this paper has the shortest running time among the four compared algorithms, which verifies the effectiveness and reliability of the algorithm of this paper.

5.3. Beam Width Comparison Analysis

When measuring the DOA estimation error in degrees, the effect of array aperture makes the error estimation inaccurate, so this experiment uses a multiple of the beam width to measure the error. A

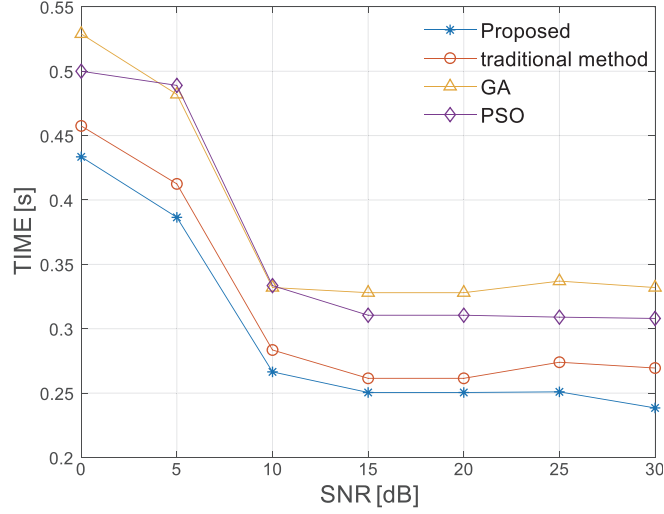


Figure 3. Average computing time of the algorithm with different SNR.

ULA with 16 sensors is considered, and the spacing of array elements is half wavelength. The SNR is 5 dB, and the number of snapshots is 512, with the selection of desired direction $\theta_k = 15^\circ$. Figure 4 represents the array orientation diagram before and after correction using different methods. The angle between the two directions where the radiated power on both sides of the main flap decreases by 3 dB is defined as the beam width. The multiplier of the beam width is defined as the ratio of the corrected beam width to the pre-corrected beam width, as shown in Table 1.

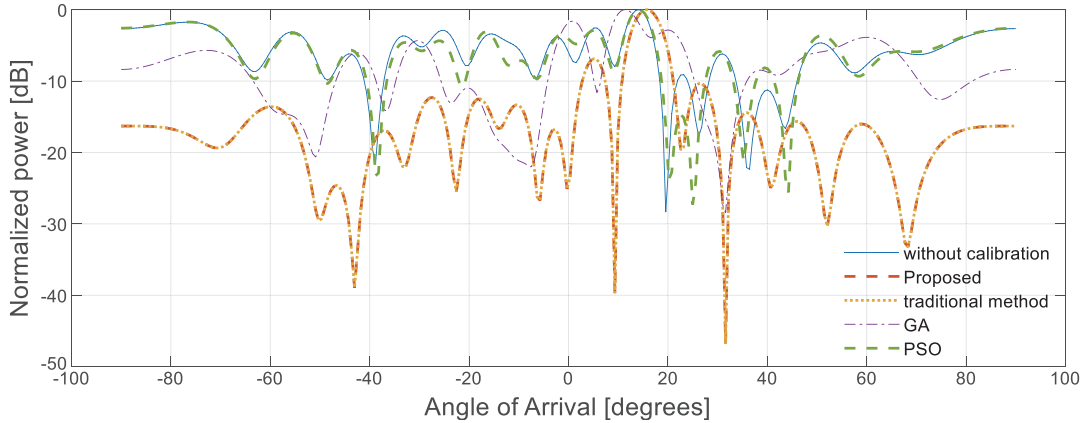


Figure 4. Array orientation diagram before and after correction by different method.

Table 1. Beam width multiplier after correction by different methods.

Proposed	GA	PSO	traditional method
0.19	0.47	0.45	0.21

The beam width is related to the antenna gain. The antenna gain describes the degree to which the antenna concentrates the power radiation, so the narrower the beam width is, the higher the gain is. As shown from Table 1, the beam width after correction by the method in this paper is the thinnest, which is 0.19 times of that before correction, indicating that the correction algorithm effectively suppresses the effect of noise and improves the antenna gain and angular resolution.

5.4. Experimental Analysis of Actual Measurement Data

The data in this paper were taken from the actual radar field measurements in the South China Sea on January 10, 2008. The antenna array is a 4×4 planar array with half times the wavelength spacing of the array elements. The array receives a group of detection signals every 4–5 minutes, and the scale of each group of received signals is $16 \times 40 \times 512$ (16 indicates the number of antennas; 40 indicates the number of distance elements; the distance resolution of the antenna array is 2.5 km; the maximum detection distance is 100 km; 512 indicates the number of snapshots). The SNR gain is defined as the difference between the signal power at the Bragg peak and the signal power in the first-order spectral region.

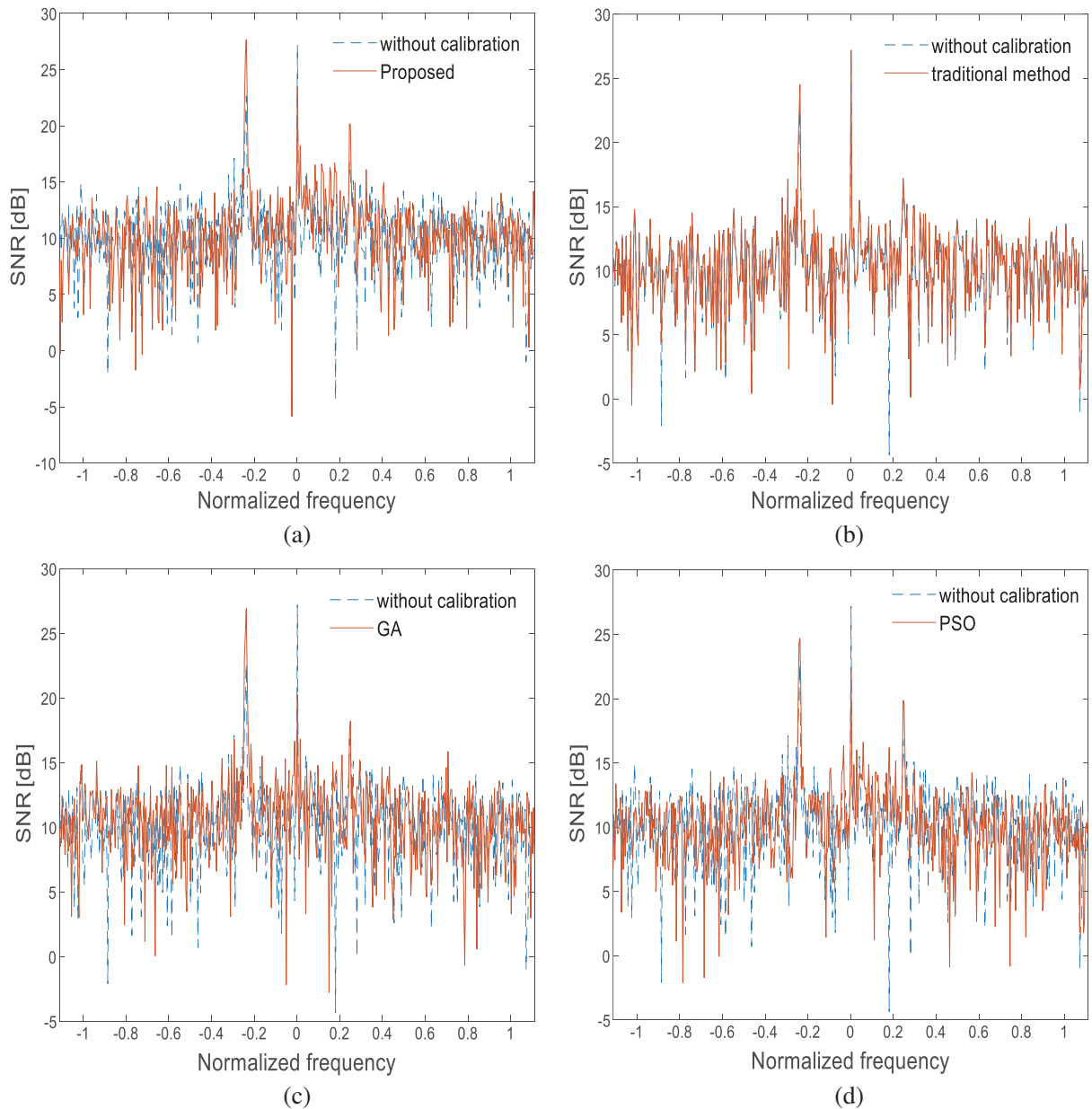


Figure 5. Spectrum map after calibration by different methods. (a) After calibration by proposed method. (b) After calibration by traditional method. (c) After calibration by GA. (d) After calibration by PSO.

The data received at 16 : 21 are selected, and the spectrum map after calibration using different methods is shown in Figure 5. It can be seen that the spectrum has been improved after the correction by different algorithms. Take a left first-order peak as an example; the spectrum value is 22.67 dB before calibration and is 27.67 dB after calibration by the algorithm of this paper. Calibration by the traditional method is 24.5 dB; calibration by GA is 26.92 dB; calibration by PSO is 24.69 dB. After calibration by the proposed algorithm, the left first-order peaks have been improved about 5 dB, which shows that the calibration method has effectively reduced the impact of noise and the gain-phase inconsistency between arrays. The SNR gain plots after the gain-phase correction compensation of 20 fields of detection data selected on January 10 using different algorithms are shown in Figure 6. The figure shows that the algorithm of this paper has higher SNR gain after correction compared with other methods, which indicates a better correction effect.

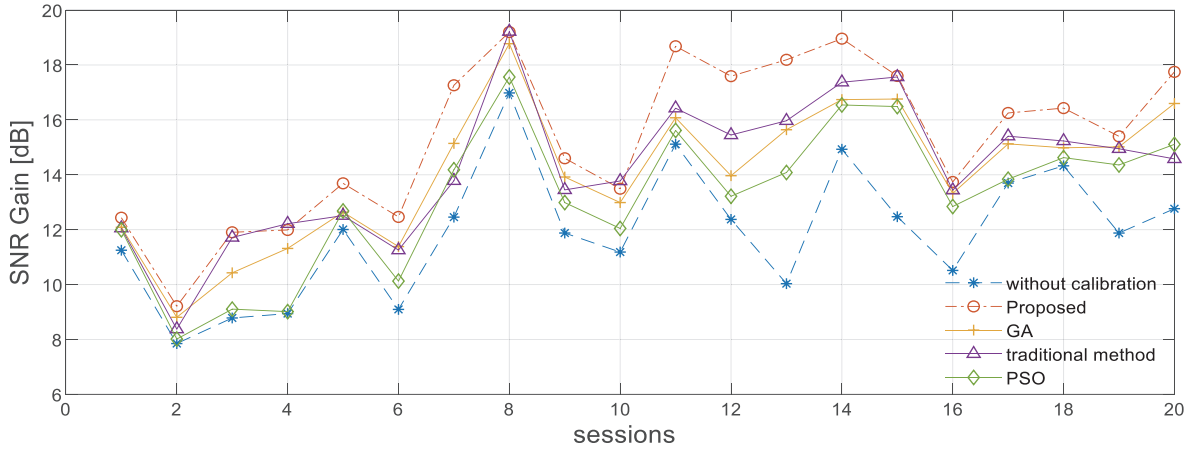


Figure 6. SNR gain before and after calibration by different methods.

The algorithm’s reliability in this paper is verified by applying the method to the DOA estimation of specific spectral points, and the obtained MUSIC space spectrum is shown in Figure 7. Figures 7(a) and (b) compare the MUSIC spatial spectrum after correction at the 313th frequency point of the 15th

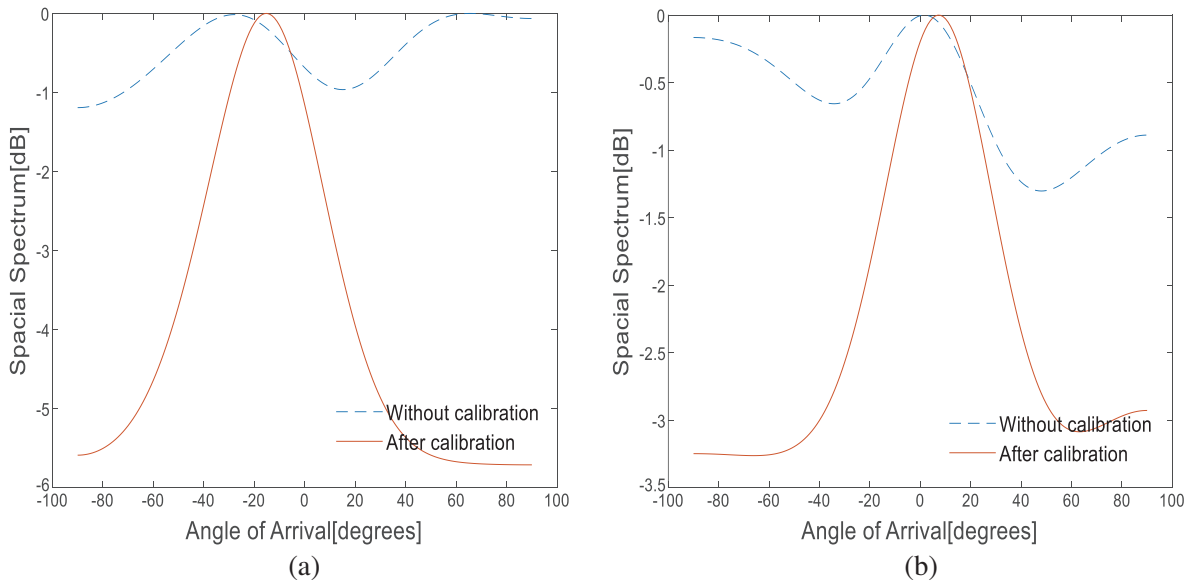


Figure 7. MUSIC spatial spectra at specific spectral points after calibration.

distance element and the 163rd frequency point of the 11th distance element of the received data at 12:05 a.m. and 2:22 p.m., respectively. From the comparison graphs, it can be seen that the MUSIC spatial spectrum before correction is relatively flat, and the information of the spectral peaks is weak, so the angular information cannot be accurately obtained when the deviation of the antenna unit is significant. After correction, the spectral peaks increase significantly, as shown in Figure 7(a), by about 5 dB, indicating that the array error correction effectively improves the SNR. The performance of DOA estimation is significantly enhanced. The DOA estimation before and after correction was performed for the above two data fields respectively, and the estimation results are shown in Figure 8.

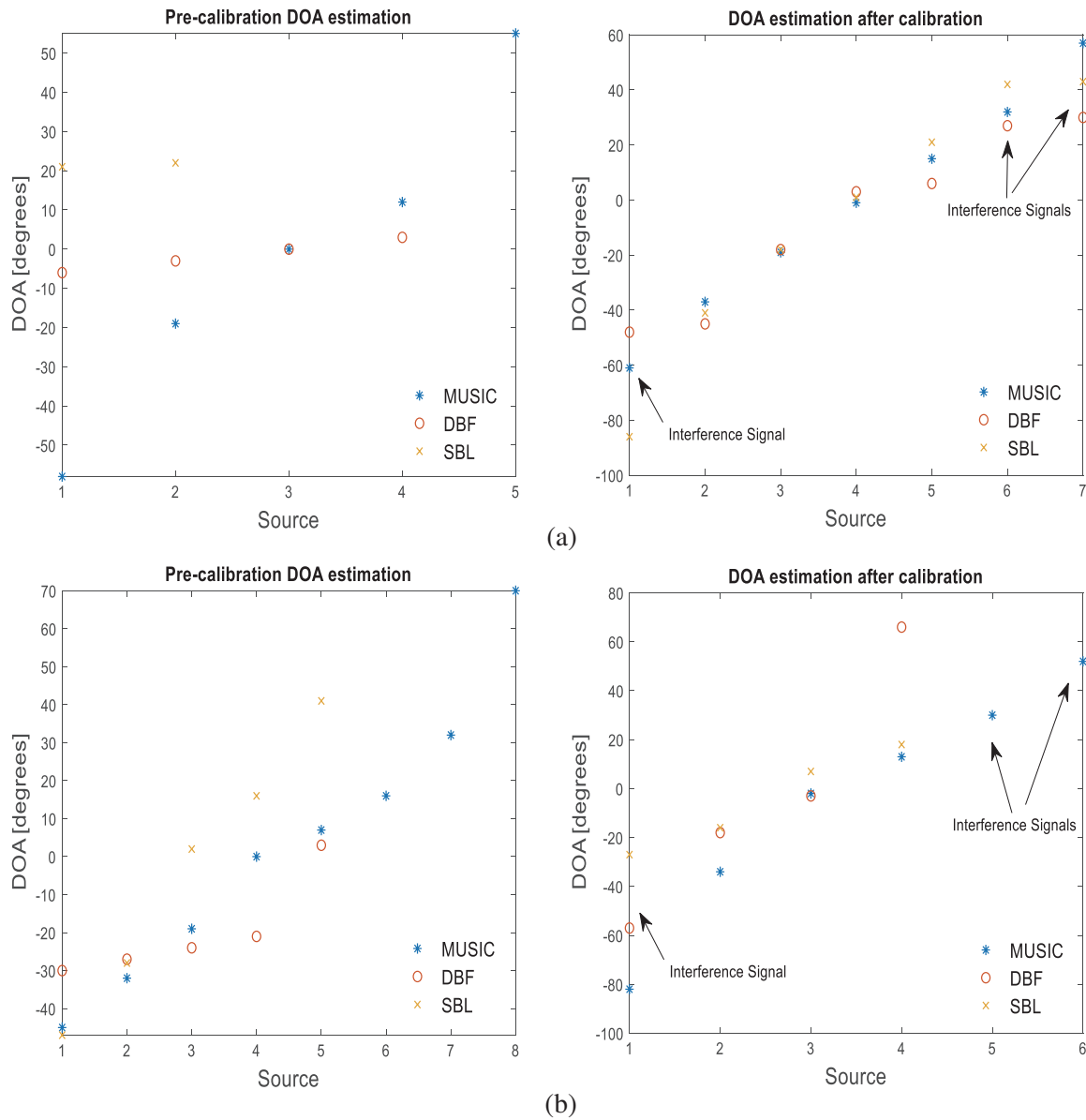


Figure 8. DOA estimation before and after calibration by different methods. (a) 12:05 a.m. 15th distance metadata. (b) 2:22 p.m. 11th distance metadata.

Due to the experimental conditions, we have not obtained the ocean buoy data values for the experimental sea area. Therefore, the algorithm’s reliability was verified by comparing whether the DOA estimates before and after data correction using different algorithms are consistent.

The function of DOA estimation is to determine the orientation of the signal, measure the direction of the selected target signal from the received data, and mark it as the source to be counted regardless of whether the desired signal is a valuable signal or an interfering signal. However, due to the low energy of the interfering signal, the result of the orientation estimation of the interfering signal has a significant error. As shown in Figure 8, the DOA obtained by the MUSIC, DBF, and Proposed method before calibration differed significantly due to the significant phase deviation. The DOA could not be accurately determined. After the calibration, the orientation estimates of the valuable signals obtained by the three methods are consistent, indicating that the corrected data can accurately estimate the incoming wave direction.

6. CONCLUSIONS

Most self-calibration algorithms are computationally intensive in solving the array error calibration coefficients, and not easy to obtain the optimal solution and easy to fall into local optimality. To address the above issues, this paper proposes a joint estimation method based on SBL for the DOA estimation and array gain-phase deviation to address the above problems. Using SBL estimation DOA produces a sparser solution with relatively low computational complexity. The estimated DOA is used as the iterative process, and the optimal solution is more easily obtained when the EM algorithm is applied to solve the deviation parameters. It is shown that the proposed algorithm can accurately find the DOA of the desired signal when the gain-phase deviation of the array exists. The accuracy is the highest among the four algorithms compared and analyzed. The antenna gain is effectively improved after correction, which further verifies the efficiency and accuracy of the passive modification of the algorithm.

REFERENCES

1. Xu, S., B. Chen, and H. Xiang, "Direction-of-arrival estimation using estimator banks in lowangle tracking for S-band radar," *Microwave and Optical Technology Letters*, Vol. 63, No. 12, 2997–3001, 2021.
2. McCloud, M. L. and L. L. Scharf, "A new subspace identification algorithm for high-resolution DOA estimation," *IEEE Transactions on Antennas and Propagation*, Vol. 50, No. 10, 1382–1390, 2002.
3. Vallet, P., X. Mestre, and P. Loubaton, "Performance analysis of an improved MUSIC DoA estimator," *IEEE Transactions on Signal Processing*, Vol. 63, No. 23, 6407–6422, 2015.
4. Wang, Y., H. Chen, and Y. Peng, *Theory of Spectrum Estimation*, The Press of Tsinghua University, Peking, 2004.
5. Liu, S., Z. Jing, and Z. Xiao, "DOA estimation with sparse array under unknown mutual coupling," *Progress In Electromagnetics Research Letters*, Vol. 70, 147–153, 2017.
6. Tian, Y., Z. Dong, and S. Liu, "Direction finding for coherently distributed sources with gain-phase errors," *Progress In Electromagnetics Research Letters*, Vol. 96, 153–161, 2021.
7. Peng, W., et al., "A joint calibration method for array gain-phase errors and mutual coupling errors," *2020 IEEE 3rd International Conference on Electronic Information and Communication Technology (ICEICT)*, IEEE, 2020.
8. Weiss, A. J. and B. Friedlander, "Array shape calibration using sources in unknown locations—a maximum likelihood approach," *IEEE Transactions on Acoustics, Speech, and Signal Processing*, Vol. 37, No. 12, 1958–1966, 1989.
9. Weiss, A. J. and B. Friedlander, "Eigenstructure methods for direction finding with sensor gain and phase uncertainties," *Circuits, Systems and Signal Processing*, Vol. 9, No. 3, 271–300, 1990.
10. Xu, Q., H.-H. Tao, and G.-S. Liao, "Array gain and phase error correction based on GA," *Systems Engineering and Electronics*, Vol. 28, No. 5, 654–657, 2006.

11. Peng, W., et al., "A joint calibration method for array gain-phase errors and mutual coupling errors," *2020 IEEE 3rd International Conference on Electronic Information and Communication Technology (ICEICT)*, IEEE, 2020.
12. Nannuru, S., et al., "Sparse Bayesian learning with multiple dictionaries," *Signal Processing*, Vol. 159, 159–170, 2019.
13. Wipf, D. P. and B. D. Rao, "Sparse Bayesian learning for basis selection," *IEEE Transactions on Signal Processing*, Vol. 52, No. 8, 2153–2164, 2004.
14. Lu, Z., et al., "Amplitude and phase errors self-correcting algorithm based on the uniform circular array," *Proceedings of 2012 2nd International Conference on Computer Science and Network Technology*, IEEE, 2012.
15. Xu, L., J. Chen, and Y. Gao, "Off-grid DOA estimation based on sparse representation and rife algorithm," *Progress In Electromagnetics Research M*, Vol. 59, 193–201, 2017.
16. Salama, A. A., M. Omair Ahmad, and M. N. S. Swamy, "Compressed sensing DOA estimation in the presence of unknown noise," *Progress In Electromagnetics Research C*, Vol. 102, 47–62, 2020.
17. Golub, G. H. and C. Reinsch, "Singular value decomposition and least squares solutions," *Linear Algebra*, 134–151, Springer, Berlin, Heidelberg, 1971.
18. Li, Y., C. Campbell, and M. Tipping, "Bayesian automatic relevance determination algorithms for classifying gene expression data," *Bioinformatics*, Vol. 18, No. 10, 1332–1339, 2002.
19. Wipf, D. P. and B. D. Rao, "An empirical Bayesian strategy for solving the simultaneous sparse approximation problem," *IEEE Transactions on Signal Processing*, Vol. 55, No. 7, 3704–3716, 2007.
20. Moon, T. K., "The expectation-maximization algorithm," *IEEE Signal Processing Magazine*, Vol. 13, No. 6, 47–60, 1996.